9C.6 THE RELATIVE ROLES OF DIABATIC AND DYNAMIC PROCESSES IN DOWNSTREAM DEVELOPMENT FOLLOWING THE EXTRATROPICAL TRANSITION OF TROPICAL CYCLONES OVER THE WESTERN NORTH PACIFIC

Elizabeth Sanabia and Patrick Harr
Department of Meteorology
Naval Postgraduate School
Monterey, CA 93943

1. INTRODUCTION

Periods of reduced forecast accuracy from operational global models often occur during the extratropical transition (ET) of tropical cyclones. Generally, the ET of a tropical cyclone involves complex interactions between the tropical cyclone (TC) and the midlatitude circulation into which it is moving. Efforts to accurately characterize these interactions have typically focused on the role of various TC- and midlatitude-related processes in the transition of the TC. Here, the focus is on the impact of these processes on the downstream development of the longwave pattern.

Downstream development can be observed in the synoptic-scale flow following ET as Rossby wave propagation of anomalous upper-level heights. Sardeshmukh and Hoskins (1988) found that excitation and propagation of upper-level Rossby waves can result from steady divergence above a tropical heat source. As a TC enters the midlatitudes during ET, the heat source is brought farther north, generating an upper-level Rossby wave response that propagates along a great circle route.

Eddy kinetic energy (EKE) analysis is an alternate method to examine wave growth and downstream development. The dispersion of eddy kinetic energy from an upstream source through ageostrophic geopotential flux (AGF) divergence provides a source of growth for downstream energy centers (Orlanski and Katzfey 1991). The upstream source here is the transitioning TC, which provides a source of EKE through AGF divergence, thereby propagating energy downstream and amplifying the longwave pattern.

Two examples of downstream development following ET in the western North Pacific are associated with the extratropical transitions of Tropical Storm (TS) Banyan in July 2005 and Typhoon (TY) Man-yi in July 2007 (Fig. 1). While each ET had a similar effect on the longwave pattern, the characteristics of each TC and their respective ETs differed significantly.

With winds that never reached typhoon intensity, Banyan maintained tropical storm intensity from 21-28 July 2005 (Fig. 2a). Forming south of Japan, the TC transited northward before turning to the northeast along Japan's east coast. Banyan began the transformation stage of the ET process at 1800 UTC 21 July 2005 and then rapidly re-intensified as an extratropical cyclone. As Banyan underwent ET, a significant midlatitude ridge developed immediately downstream.

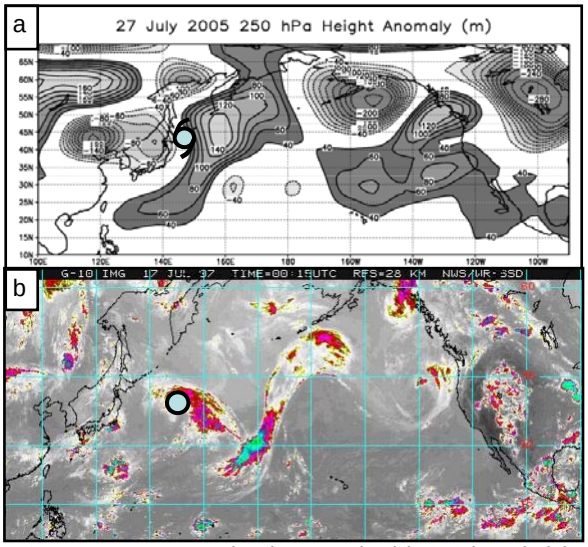

FIG. 1. Downstream development in (a) 250-hPa height anomalies (m) for 0000 UTC and 1200 UTC 27 July 2005 illustrating the Rossby wave-like response following the ET of TS Banyan (from Harr and Dea 2008). (b) Water vapor image from Geostationary Operational Environmental Satellite-10 (GOES-10) depicting the Rossby wave-like pattern originating from the ex-Man-yi and extending east northeastward throughout the North Pacific at 0000 UTC 17 July 2007. The tropical cyclone symbol marks the location of TS Banyan at 1200 UTC 27 July 2005. The shaded circle depicts the position of the extratropical storm resulting from Man-yi.

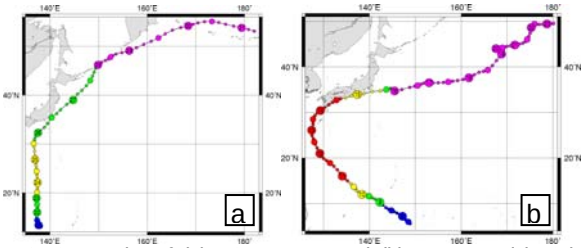

FIG. 2. Tracks of (a) TS Banyan and (b) TY Man-yi in 3-h increments with color-coding defined as: blue indicates tropical depression (international class 2), green indicates tropical storm (int'l. class 3, JMA Typhoon), yellow indicates severe tropical storm (int'l. class 4), red indicates typhoon (int'l. class 5) and magenta indicates an extratropical cyclone (int'l. class 6) (from: http://agora.ex.nii.ac.jp/digital-typhoon/).

Corresponding author address: Elizabeth R. Sanabia, Dept. of Meteorology, Naval Postgraduate School, Monterey, CA 93943-5119; email: ersanabi@nps.edu

By contrast, TY Man-yi was a super typhoon and followed the classic "C"-shaped ET track (Fig. 2b). Man-yi maintained TC intensity from 09-16 July 2007, and began the transformation stage of ET at 0800 UTC 14 July 2007. Also in contrast to Banyan, Man-yi recurved beneath a developing midlatitude ridge. The adjacent ridge downstream of Man-yi while present was not significant. The dominant local feature was the midlatitude trough that developed and deepened through the ET period.

While the dominant midlatitude feature that developed immediately downstream of the TC during each ET differed, (a ridge in the Banyan case and a trough in the Man-yi case), the impact of each ET was the same – downstream development across the entire North Pacific. Therefore, it is hypothesized that the evolution of the ET in these two cases represents two possible pathways to downstream development.

It is proposed that the significant amplitude and scale of the midlatitude feature that developed in the local environment of the decaying TC played a critical role in determining the response of the synoptic circulation downstream. Also, the evolution of the local response, (a ridge in the Banyan case and a trough in the Man-yi case), was primarily influenced respectively by lower-level and upper-level mechanisms during each ET process.

The primary physical mechanisms that enhance development of the adjacent midlatitude ridge are warm air advection (WAA) and latent heat release (LHR). A maximum at low levels, WAA enhances the slantwise ascent of warm moist air and is most prominent along the eastern side of the TC during ET. Latent heat release results from condensation of this moist air during its ascent and this diabatic process typically occurs at midlevels in the troposphere.

The two primary physical mechanisms that act in concert to help deepen the adjacent midlatitude trough are the midlatitude jet and the TC outflow. The TC outflow can couple favorably with a divergent quadrant of the midlatitude jet to enhance upward vertical motion and lower surface pressure.

Comparison of these key features during the TC-midlatitude interaction in these two cases will enable continued progress toward understanding the physical mechanisms during ET that govern wave amplification and development downstream.

2. METHOD

A diagnostic study of TS Banyan and TY Man-yi was conducted consisting of synoptic, satellite, EKE and PV analyses. Critical factors during TC-midlatitude interaction were examined for both TS Banyan and TY Man-yi to determine their relative roles and impact on the evolution of the midlatitude feature immediately downstream of the ET.

The Global Data Assimilation System (GDAS) output at one degree latitude/longitude resolution was used to examine the evolution of the synoptic-scale circulation and the local and downstream responses to each ET event. The GDAS analysis and 6-hr forecast fields are the last of the operational model runs at the National Centers for Environmental Prediction (NCEP), and they incorporate late observational data not included in the earlier operational runs.

Satellite data were used to evaluate the thermal structure of the local environment in each case. Microwave satellite data from the Advanced Microwave Sounding Unit-A (AMSU-A) were used to define temperature profiles during the ET of both Banyan and Man-yi.

Eddy kinetic energy budgets were evaluated to determine the quantitative contribution of the TC to the growth of the midlatitude wave pattern. Additionally, the volume-integrated EKE was evaluated by area following both ETs to assess the eastward movement of EKE across the Pacific basin over time.

Potential vorticity analyses were utilized to assess the evolution of the local response to the TC-midlatitude interaction. Fields at each critical time were examined in a PV framework. The evolution of PV associated with features of interest (i.e. the negative anomaly associated with the adjacent ridge for Banyan and the positive anomaly associated with the adjacent trough for Man-yi) were examined to define relative phasing, amplitudes and interaction. These analyses were focused on the roles associated with generating forcing of downstream development.

3. ANALYSIS

Tropical storm Banyan (2005/07W) first reached tropical storm strength at 1800 UTC 21 July 2005. A fairly weak storm, Banyan's maximum sustained winds were 55 kts and minimum pressure was 975 hPa. Following ET, Banyan underwent reintensification and became an intense extratropical system at 0000 UTC 28 July 2005. The ET of Banyan also elicited downstream development in the form of Rossby waves, evident in the 250-hPa-anomaly chart in Fig. 1a (Harr and Dea 2008).

Prior to Banyan's movement into the midlatitudes, a low-pressure center over the Aleutian Islands was the dominant feature in the North Pacific. Secondary troughing was in place over the northeast Asian seaboard, and a cutoff low was located east of Japan between a weak western Pacific ridge to the north and the subtropical ridge to the south. At 0000 UTC 25 July 2005 (Fig. 3a), Banyan tracked northward along the western boundary of the subtropical ridge and approached the eastern side of the trough along the Asian seaboard. At upper levels, the primary midlatitude jet was located between 40^{o}N -50^{o}N.

The trough amplified over the Sea of Japan as Banyan continued heading northeast at 13 kts at 0000 UTC 26 July 2005 (Fig. 3b). East of Banyan, a weak ridge developed, separating the transitioning TC

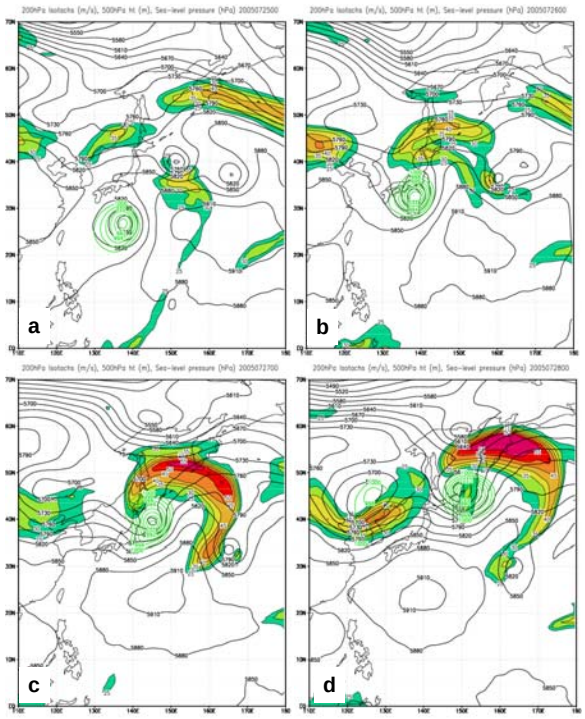

FIG. 3. Contours of 500 hPa height (m, black lines), sea-level pressure (hPa, green lines), and wind speed at 200 hPa (m s-1, shaded) during the ET of TS Banyan at (a) 0000 UTC 25 July 2005, (b) 0000 UTC 26 July 2005, (c) 0000 27 July 2005, and (d) 0000 UTC 28 July 2005.

from the weak upper-level low-pressure system. As Banyan moved into the midlatitudes, the upper-level outflow became adjacent to the midlatitude jet (Fig. 3b).

By 0000 UTC 27 July 2005 (Fig. 3c), TS Banyan had fully merged with the midlatitude trough. The adjacent downstream ridge continued to develop and the height gradient increased with the low height center at 165°E. By this time, the outflow from Banyan and the midlatitude jet merged and acquired a pronounced anticyclonic curvature as the upper-level ridge continued to amplify east of Banyan.

By 0000 UTC 28 July 2005, Banyan had completed ET (Fig. 3d). The ex-Banyan deepened significantly into an intense extratropical system. The ridge just east of Banyan continued to build just west of the dateline and the cutoff low that had been to its south began to dissipate. Although the anticyclonic curvature of the upper-level jet northeast of the ex-Banyan circulation decreased, the intensity of the jet was maintained.

Assessing total kinetic energy, Harr and Dea (2008) were able to track the eastward propagation of EKE following the ET of Banyan (Fig. 4). The increase in EKE through the basin over time is evidenced by the successive peaks (western, central, then eastern Pacific) in EKE between 28-31 July. Harr and Dea (2008) also determined that the downstream increase in EKE was due primarily to AGF convergence.

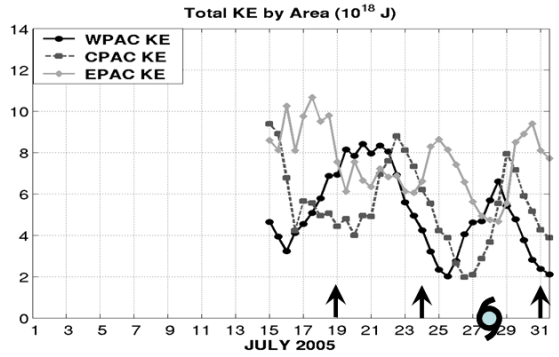

FIG. 4. Volume integrated eddy kinetic energy (1018 J) over the North Pacific between 15-31 July 2005. The TC symbol marks the date that TS Banyan moved poleward of 40°N. The arrows mark the last date associated with other tropical cyclones that stayed south of 40°N (from Harr and Dea 2008).

The case of TS Banyan illustrates the development of a Rossby-wave response and downstream development following ET. Although Banyan was a weak TC, the development of a strong anticyclone immediately downstream of Banyan contributed to the perturbation of the midlatitude flow (Vancas 2006).

Typhoon Man-yi (2007/04W) first reached tropical storm strength at 0000 UTC 9 July 2007. After tracking northwestward for three days, Man-yi experienced 24 hours of 95-kt maximum sustained winds and 930-hPa minimum pressures prior to the eye passing over Okinawa at 0000 UTC 13 July 2007. Man-yi then began to recurve, heading due north for 12 hours, then east-northeast along the Japanese coast. Man-yi continued east northeastward even after it completed extratropical transition at 0000 UTC 16 July 2007. Man-yi's ET produced a significant longwave response that is displayed in the water vapor satellite image in Fig. 1b. The longwave pattern contributed to a rare midsummer cyclone over northern California.

At 0000 UTC 13 July 2007 (Fig. 5a), a large ridge existed over eastern Asia. Zonal flow extended over Japan and offshore to the east in association with a digging trough to the northeast. Man-yi was located over Okinawa (26°N, 127.4°E), heading north at 11 kts along the western boundary of the subtropical ridge toward the right entrance region of the jet above mainland Japan.

At 0000 UTC on 14 July 2007 (Fig. 5b), ridging continued over eastern Asia. The split jet flow around the ridge over eastern Asia merged offshore east of Japan. This contributed to an increase in the jet maximum and deepening of the trough at 160°E. Man-yi was located over southwestern Japan, tracking northeast at 11 kts along the northwest corner of the subtropical ridge with the East Asian ridge well to the north.

Twenty-four hours later, at 0000 UTC 15 July 2007 (Fig. 5c), the ridge over northeastern Asia weakened slightly as Man-yi passed beneath the ridge axis. The primary trough east of Japan continued to deepen. Although the upper-level center

continued to move eastward, the relative jet maximum remained centered near 155°E as it merged with the outflow from TY Man-yi. A 500-hPa shortwave northeast of Man-yi (located at 42°N, 152°E) began to drop southward east of Man-yi.

By 0000 UTC 16 July 2007 (Fig. 5d), Man-yi completed ET and continued to track east-northeastward. The upper-level shortwave that had been northeast of Man-yi 24-h earlier (Fig. 5c) had now dropped into the primary trough and amplified directly east of the ex-Man-yi. The relative maximum in the upper-level jet maintained a position east of Man-yi and continued to lead into the base of the trough along 165°E. As Man-yi underwent ET, an upper- level Rossby wave-like response became clear in satellite imagery (Fig. 1b).

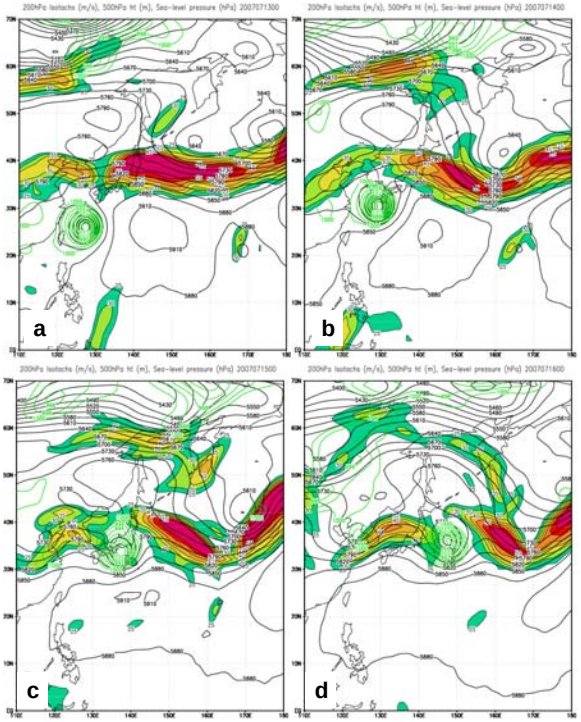

FIG. 5. Contours of 500 hPa height (m, black lines), sea-level pressure (hPa, green lines), and wind speed at 200 hPa (m s-1, shaded) during the extratropical transition of TY Man-yi at (a) 0000 UTC 13 July 2007, (b) 0000 UTC 14 July 2007, (c) 0000 15 July 2007, and (d) 0000 UTC 16 July 2007.

Although the ET of TS Banyan and TY Man-yi resulted in amplification of a Rossby wave-like pattern downstream, there were clear differences in the impact of each case on the synoptic-scale flow over the western North Pacific. The ET of TS Banyan was associated with the rapid amplification of an anticyclone immediately adjacent to the ET. The combination of the ridge amplification and merger of TC outflow and midlatitude flow resulted in a strong jet with pronounced anticyclonic curvature immediately downstream of Banyan.

In the case of Man-yi, the merger of TC outflow and midlatitude flow occurred in association with a digging trough immediately downstream of the ET. Although a slight ridge built east of Man-yi, the western North Pacific was dominated by the digging trough and jet maximum that was extending from the outflow of Man-yi to the base of the trough. The cases of Banyan and Man-yi suggest that the pathway to development of a downstream pattern contains a large amount of variability.

4. DISCUSSION

The objective of this research is to identify and understand the physical mechanisms during ET that govern wave amplification and development downstream. Increased understanding of the mechanisms that impact downstream development will reduce the uncertainty and increase the predictability associated with downstream development following ET.

It is hypothesized that there are three possible pathways to downstream development following an ET event. Furthermore, each pathway is associated with a specific physical mechanism and the dominant pathway depends on the phasing between the decaying TC and the midlatitude flow into which it is moving. Finally, an unfavorable phasing between the decaying TC and the midlatitude flow would sufficiently degrade the physical mechanisms associated with all pathways such that no downstream impact occurs.

In the diabatic pathway, strong low-level warm air advection leads to amplification of an upper-level anticyclone (Parker and Thorpe 1995; Wernli et al. 2002; Moore and Montgomery 2004, 2005) and is hypothesized to initiate the downstream response. This pathway is typified by the case of TS Banyan in which downstream development was attributed to the anticyclone that developed adjacent to and immediately downstream from Banyan (Vancas 2006). The adjacent anti-cyclone developed as a result of favorable phasing of the TC with the midlatitude flow, which enabled the warm-air advection, slantwise ascent and latent-heat release on the east side of Banyan to complement the building midlatitude ridge in the destruction of potential vorticity (PV) at upper levels and an increase in PV at low levels (Fig. 6).

In the dynamic pathway, the outflow of the TC is directly connected to a developing upper-level trough immediately downstream of the ET. The quickly amplifying trough initiates the downstream response. In Typhoon Man-yi, unfavorable phasing between the TC and the midlatitude flow resulted in the separate development of the ridge in the midlatitude flow and the weak anticyclone due to the TC outflow, yet downstream development still occurred. The proposed cause of downstream development in this case was the downstream propagation of kinetic energy from the trough that deepened due to the combination of the TC outflow, the proximity of the TC to the right entrance quadrant

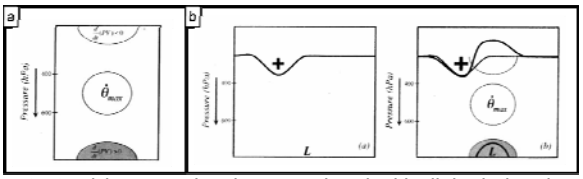

FIG. 6. (a) PV tendencies associated with diabatic heating. The circle labeled $\dot{\theta}_{\max}$ is the diabatic-heating maximum. The light (dark) shading above (below) it indicates the region of PV destruction (production). (b) Diabatic heating within the context of a developing cyclone. Left: relationship between an upper-tropospheric PV anomaly (+ sign) and a surface low-pressure center ('L'). Right: Ascent downstream of the PV anomaly produces latent heat release manifest as a $\dot{\theta}_{\max}$. The erosion of PV aloft deforms the bold PV contour to the east of the original anomaly, making that anomaly even more anomalous (larger + sign). The production of PV in the lower troposphere intensifies the surface cyclone with high values of PV developing near the center indicated by the bold black line surrounding the 'L' (from Martin 2006).

of the jet, and the merger of split jet flow into a single midlatitude jet.

In the combination pathway, strong low-level warm-air advection occurs in a region that is located in a favorable quadrant of an upper-level jet such that strong Rossby wave-like development downstream occurs in conjunction with a strong re-intensification of the decaying TC as an extratropical system. The upper- and lower-level PV anomalies phase-lock, as in a baroclinic environment, and result in the subsequent self-amplification of that system (Hoskins et al. 1985).

The three pathways may be characterized as being dominated by low-level conditions (diabatic case), upper-level conditions (dynamic case), and the combination of upper and low levels (combination case) as is typical in Petterssen Type B development. Additionally, all three pathways result in significant modification of the midlatitude flow in the local region in which the ET occurs.

It is theorized that the common increase in amplitude of the local environmental pattern drives the downstream response, as ageostrophic geopotential fluxes act to disperse EKE downstream, which increases the amplitude of the downstream wave (Orlanski and Katzfey 1991; Orlanski and Chang 1993; Chang 1993; Orlanski and Sheldon 1993, 1995.) It is hypothesized that the kinetic energy impulse that results from the amplification of the near-field midlatitude pattern may be transported downstream in all three pathways, which amplifies the longwave pattern in the far field and results in downstream development.

These three pathways may be placed in a PV framework. In the diabatic case, a negative PV anomaly is built aloft and low-level positive PV anomaly occurs due to the diabatic processes (Fig. 6) associated with the warm-air advection and warm frontogenesis east of the decaying TC. In the dynamic case, an upper-level positive PV anomaly is found immediately downstream of the decaying TC. No appreciable low-level PV anomaly exists in the dynamic case. In the combination case, the interaction of upper-level and lower-level PV anomalies occurs as defined by Hoskins et al. (1985) in association with a Petterssen Type B development. Mutual interaction takes place between a low-level positive PV anomaly, which results from the combination of the decaying TC and the warm air advection (as defined in the diabatic case), and an upper-level positive PV anomaly, which results from the approach of a pre-existing upper-level trough upstream of the decaying TC (Klein et al. 2002, Ritchie and Elsberry 2003, McTaggart-Cowan et al. 2001).

It is hypothesized that certain thresholds for the magnitude, phasing, and duration of PV anomalies that correspond to key features for each mechanism exist and must be met or exceeded to amplify the local midlatitude pattern and elicit a downstream response. For example, there may be a minimum value of the low-level positive PV anomaly corresponding to warm-air advection (key feature for the low-level diabatic mechanism) that is necessary to build a ridge of sufficient amplitude to initiate a downstream response. Furthermore, the characteristics of the PV anomalies associated with the mechanisms that define each pathway will impact the downstream propagation of EKE. A key point associated with this hypothesis is the establishment of a sensitivity of downstream development to the characteristics associated with each pathway.

ACKNOWLEDGMENTS

This research is funded by the National Science Foundation Climate and Large-Scale Dynamics and the Office of Naval Research, Marine Meteorology.

REFERENCES

Harr, P. A., and J. M. Dea, 2008: Downstream development associated with the extratropical transition of tropical cyclones over the western North Pacific. *Mon. Wea. Rev*., in press.

Hoskins, B. J., M. E. McIntyre, and A. W. Robertson, 1985: On the use and significance of isentropic potential vorticity maps. *Quart. J. Roy. Meteor. Soc*., **111**, 877-946.

Klein, P. M., P. A. Harr, and R. L. Elsberry, 2002: Extratropical transition of western North Pacific tropical cyclones: Midlatitude contributions to intensification. *Mon. Wea. Rev.*, **130**, 2240-2259.

Martin, J. E., 2006: *Mid-Latitude Atmospheric Dynamics: A First Course*. John Wiley & Sons, Ltd, 324 pp.

McTaggart-Cowan, R., J. R. Gyakum, and M. K. Yau, 2001: Sensitivity testing of extratropical transitions using potential vorticity inversions to modify initial conditions: Hurricane Earl case study. *Mon. Wea. Rev., **129**, 1617-1636.*

Moore, R. W., and M. T. Montgomery, 2004: Reexamining the dynamics of short-scale, diabatic Rossby waves and their role in midlatitude moist cyclogenesis. *J. Atmos. Sci.*, **61**, 754-768.

----, and ----, 2005: Analysis of an idealized, three-dimensional diabatic Rossby vortex: A coherent structure of the moist baroclinic atmosphere. *J. Atmos. Sci.*, **62**, 2703-2725.

Orlanski, I., and J. Katzfey, 1991: The life cycle of a cyclone wave in the Southern Hemisphere. Part I: Eddy energy budget. *J. Atmos. Sci.*, **48**, 1972-1998.

----, and E. K. M. Chang, 1993: Ageostrophic geopotential fluxes in downstream and upstream development of baroclinic waves. *J. Atmos. Sci.*, **50**, 212-225.

----, and J. Sheldon, 1993: A case of downstream baroclinic development over western North America. *Mon. Wea. Rev.*, **121**, 2929-2950.

----, and ----, 1995: Stages in the energetics of baroclinic systems. *Tellus*, **47A**, 605-628.

Parker, D. J., and A. J. Thorpe, 1995: Conditional convective heating in a baroclinic atmosphere: a model of convective frontogenesis. *J. Atmos. Sci.*, **52**, 1699-1711.

Ritchie, E. A., and R. L. Elsberry, 2003: Simulations of the extratropical transition of tropical cyclones: Contributions by the midlatitude upper-level trough to reintensification. *Mon. Wea. Rev.*, **131**, 2112-2128.

Sardeshmukh, P.D. and B. J. Hoskins, 1988: The generation of global rotational flow by steady idealized tropical divergence. *J. Atmos. Sci.*, **45**, 1228-1251.

Vancas, M. D., 2006: The extratropical transition of Tropical Storm Banyan. M. S. thesis, Dept. of Meteorology, Naval Postgraduate School, 72 pp.

Wernli, H., S. Dirren, M. A. Liniger, and M. Zillig, 2002: Dynamical aspects of the life cycle of the winter storm 'Lothar' (24-26 December 1999). *Quart. J. Roy. Meteor.* Soc., **128**, 405-429.